International Journal of Zoology and Applied Biosciences
Volume 10, Issue 6, pp: 117-134, 2025
https://doi.org/10.55126/ijzab.2025.v10.i06.013
ISSN: 2455-9571
http://www.ijzab.com
Research Article

APOPTOSIS- INDUCING AND CYTOTOXICITY POTENTIAL OF ETHANOLIC FLOWER EXTRACT *COMBRETUM INDICUM A*GAINST HUMAN RETINOBLASTOMA (Y79) CELLS VALIDATED BY *IN VITRO* AND *IN SILICO* DOCKING STUDIES

[1]Kattumuchikkal Sidharth, [2*]Narayanasamy Kandhasamy, [1]Nirmala Devi and [3]Sruthy Mohan

[1]Department of Biochemistry, Sree Narayana Guru College, Coimbatore - 641105, Tamil Nadu, India
[2*]Department of Food science and Nutrition, Nehru Arts and Science, Coimbatore - 641105, Tamil Nadu, India
[3]Department of Microbiology, Nehru Arts and Science College, Coimbatore - 641105, Tamil Nadu, India

Article History: Received 11th September 2025; Accepted 23rd October 2025; Published 1st November 2025

ABSTRACT

This study investigates the phytochemical composition, antioxidant potential, molecular interactions, and anticancer activity of the ethanolic flower extract derived from *Combretum indicum*. Qualitative analysis showed a rich presence of alkaloids, flavonoids, terpenoids, phenolic compounds, and quinones, alongside moderate amounts of saponins, cardiac glycosides, and steroids. The extract demonstrated concentration-dependent antioxidant activity in both the Ferric Reducing Antioxidant Power and phosphomolybdenum assays, showing IC_{50} values of 150 and 106.78 µg/mL, respectively. Major phytoconstituents, such as α-amyrin, 6-cyanoquinoline, supraene, trans-linalool, n-hexadecanoic acid, and hentriacontane, performed molecular docking studies with retinoblastoma protein (Rb, PDB ID: 3N5U). α-Amyrin exhibited the highest binding affinity (–8.6 kcal/mol), exceeding that of the standard drug methotrexate, indicating considerable inhibitory potential. In vitro cytotoxicity assays carried out on Y79 retinoblastoma cells demonstrated a dose-dependent decrease in cell viability (IC_{50} = 118.07 µg/mL), along with morphological alterations indicative of apoptosis. AO/EB dual staining, Annexin V/PI flow cytometry, and DNA fragmentation assays validated that apoptosis is the primary mechanism of cell death. The findings suggest that *C. indicum* flower extract, especially α-amyrin, has strong antioxidant and anticancer effects, emphasizing its potential as a natural treatment option for retinoblastoma.

Keywords: *Combretum indicum*, Molecular docking, Y79 retinoblastoma cells, Cytotoxicity, DNA fragmentation analysis.

INTRODUCTION

Retinoblastoma is the most prevalent intraocular tumor in children, originating from the inner retinal layer where the optic nerves are embedded and commonly developing within the eyeball. The disease is mainly diagnosed in early childhood, with the average age at diagnosis being around two years, and about 80% of cases are recognized before the age of three. Tumor development can infrequently occur by the age of six or seven years (Jin *et al.,* 2017; Jin *et al.,* 2024). The primary objectives of retinoblastoma treatment are to ensure survival and, thereafter, to protect the eye and visual capabilities. Each year, around 8,000 new cases are reported worldwide, with a higher prevalence observed in Asia and Africa (Dimaras *et al.,* 2015). In several cases, chemotherapy given prior to or following enucleation is essential to prevent systemic spread or involvement of the central nervous system (Zhao *et al.,* 2011; Yanik *et al.,* 2015). Whereas existing treatments typically achieve these targets, they are associated with considerable side effects and financial challenges, underscoring the importance of alternative therapeutic strategies (Doğan *et al.,* 2025).

Plants were originally used as a source of medicinal compounds, and phytochemicals continue to provide exciting potential for new therapies (Chaachouay and Zidane, 2024). A significant portion of the global

*Corresponding Author: Narayanasamy Kandhasamy, Department of Food science and Nutrition, Nehru Arts and Science, Coimbatore - 641105, Tamil Nadu, India. Email: harikns.2005@gmail.com

population, 85–90%, continues to depend on traditional medicine, whereas modern pharmaceuticals commonly depend on crude or standardized plant extracts or isolated bioactive compounds (Nasim *et al.,* 2022). Phytochemicals can be classified into primary metabolites, which consist of sugars, amino acids, proteins, and chlorophyll, and secondary metabolites, which include alkaloids, terpenoids, phenolics, flavonoids, tannins, glycosides, and saponins. These compounds demonstrate a variety of biological activities: alkaloids have analgesic and antimalarial effects; terpenoids demonstrate antiviral and anticancer properties; saponins reduce cholesterol levels and exhibit antiviral activity; glycosides inhibit fungi and bacteria; and phenols and flavonoids act as antioxidants and anti-allergic agents (Moteriya *et al.,* 2015).

Medicinal plants are currently increasingly investigated for their anticancer potential, owing to their inherent antioxidant and antibacterial properties. *Combretum indicum* (syn. *Quisqualis indica*), known as Rangoon creeper, is a rapidly growing woody vine that originates from tropical Asia, including regions such as India, the Philippines, and China. Traditionally, it has been utilized for the treatment of infections, fever, gastrointestinal problems, and skin disorders (Jain *et al.,* 2019). Phytochemical analyses have revealed the presence of bioactive constituents, including quisqualic acid, sterols, flavonoids, alkaloids, glycosides, and tannins (Yadav and Agarwala, 2011). Additionally, the plant demonstrates a range of properties, such as anti-inflammatory, antibacterial, antioxidant, anthelmintic, antiviral, antidiabetic, antihyperlipidemic, anticancer, and neuroactive effects (Monica *et al.,* 2024) a variety of these findings, its effectiveness against human retinoblastoma has not been thoroughly explored.

This study evaluated the phytochemical composition of ethanolic flower extracts from *C. indicum* and assessed their antioxidant potential. Molecular docking studies were also performed to investigate the interactions between the identified bioactive compounds and retinoblastoma-related target proteins. The extract's cytotoxic and pro-apoptotic effects on Y79 retinoblastoma cells were evaluated through MTT viability assays, AO/EB dual staining, Annexin V/PI flow cytometry, and DNA fragmentation analysis.

MATERIALS AND METHODS

Sample Collection and Preparation of Flower Extract

The *C. indicum* flowers that were collected from Ottapalam, Palakkad, Kerala, obtained authentication from the Botanical Survey of India, Coimbatore. The samples had been pulverized, cleaned, and shade-dried. The dried powder was extracted with ethanol at a 10% concentration. The extracts had been incubated at 40°C for 24 h in a rotary shaker (60–70 RPM) and were subsequently filtered. The filtrates were used for further analysis.

Phytochemical Analysis

Qualitative Analysis

The ethanolic extracts of *C. indicum* flowers went through preliminary phytochemical screening according to the standard procedures established by Gupta *et al.* (2010), which confirmed the presence of saponins, flavonoids, steroids, alkaloids, terpenoids, quinones, cardiac glycosides, phenols, fats and oils, proteins, and carbohydrates.

Antioxidant Activity Assays

FRAP (Ferric Reducing Antioxidant Power) assay

The antioxidant activity of the ethanolic flower extract of *C. indicum* was determined using the FRAP assay (Benzie *et al.,* 1996). Briefly, 0.5 mL of the extract was placed in a 1.5 mL Eppendorf tube, followed by the addition of 0.2 mL phosphate buffer (0.2 M, pH 6.6) and 1.0 mL potassium ferricyanide (0.1%). The mixture was incubated at 50°C for 20 min, after which 1.25 mL of trichloroacetic acid (TCA) was added. Samples were centrifuged at 5000 rpm for 10 min, and the supernatant was collected. To 0.5 mL of this supernatant, 0.5 mL of deionized water and 0.1 mL of ferric chloride (0.1%) were added. Absorbance was measured at 700 nm by monitoring the formation of Perl's Prussian blue complex. Reducing power was expressed as mg gallic acid equivalent per gram extract (mg GAE/g).

Phosphomolybdenum assay

Total antioxidant capacity was evaluated by the phosphomolybdenum method (Mishra *et al.,* 2021). A reaction mixture containing 0.5 mL extract and 0.5 mL reagent solution (0.6 M H_2SO_4, 28 mM sodium phosphate, 4 mM ammonium molybdate) was prepared. The mixture was incubated in a water bath at 50°C for 90 min. After cooling, absorbance was recorded at 695 nm using a Labtronics LT-291 UV–Vis spectrophotometer. Distilled water served as control. Antioxidant capacity was calculated using the following formula:

$$\text{Antioxidant effect (\%)} = \frac{\text{Absorbance Cont - Absorbance of Sample}}{\text{Absorbance Control}} \times 100$$

In silico Prediction of Potential Bioactivity

Target selection and databases

The potential bioactivity of the ethanolic flower extract of *C. indicum* against selected cancer-related proteins was evaluated *in silico*. Protein structures were retrieved from the RCSB Protein Data Bank (https://www.rcsb.org), and phytochemical ligand structures were obtained from the PubChem database (https://pubchem.ncbi.nlm.nih.gov).

Software and tools

Molecular docking studies were performed using PyRx with AutoDock Vina 0.8 (Dallakyan and Olson, 2015). Protein–ligand interactions and binding conformations were further visualized and analyzed using BIOVIA Discovery Studio Visualizer (RRID:SCR_015651) (Pawar and Rohane, 2021).

Preparation of Protein

The three-dimensional crystal structure of the retinoblastoma (Rb) protein (PDB ID: 3N5U) was retrieved from the RCSB Protein Data Bank (https://www.rcsb.org/) for docking analysis (**Figure 1**). Structural refinement was performed to optimize the protein for computational studies. The prepared protein structure was subsequently converted into PDBQT format for molecular docking simulations.

Figure 1. 3D structure representation of cancer target proteins Rb (PDB: 3N5U).

Preparation of Ligands

The ethanolic flower extract of *C. indicum* was subjected to GC–MS analysis, which led to the identification of six bioactive compounds (Sidharth *et al.,* 2024). Their chemical structures, along with that of the reference drug methotrexate (PubChem CID: 126941), are presented in Figure 2a–g. Three-dimensional conformations of the identified ligands and the standard drug were retrieved and employed in molecular docking studies to evaluate their binding potential against the retinoblastoma protein (Rb; PDB ID: 3N5U). Site-specific docking was performed, and the resulting protein–ligand complexes were systematically analyzed using the Protein–Ligand Interaction Profiler (PLIP v1.1.1). This tool provided a comprehensive characterization of the interaction networks, enabling a detailed assessment of the binding patterns and potential anticancer relevance of the compounds.

Molecular Docking

The bioactive compounds found through GC–MS analysis conducted molecular docking studies to assess their potential interactions with the retinoblastoma protein (Rb), an essential target in cancer progression (Suhaibun *et al.,* 2020). Docking simulations were conducted with AutoDock Vina within the PyRx 0.8 platform to anticipate the binding orientations and affinities of the ligands with the target protein (Eberhardt *et al.,* 2021). The three-dimensional structure of the Rb receptor (PDB ID: 3N5U) was acquired from the Protein Data Bank, and the ligands were sourced from PubChem and transformed into PDBQT format for docking procedures. A grid box was established around the receptor's active site to ensure accurate docking computations. The binding affinities of the ligands were represented as binding energies in kilocalories per mole (kcal/mol). The values estimate the intensity and stability of ligand–protein complexes, with lower (more negative) binding energies signifying stronger interactions (Ramalingam *et al.,* 2023). The docking outcomes, encompassing the binding scores, are presented in Table 1. Post-docking analysis was conducted with BIOVIA Discovery Studio Visualizer, facilitating an in-depth assessment of the ligand–protein interactions, including hydrogen bonds, hydrophobic contacts, and additional non-covalent interactions. The similar procedure was utilized for the standard drug, methotrexate, to facilitate a comparative assessment of binding efficiencies and interaction patterns.

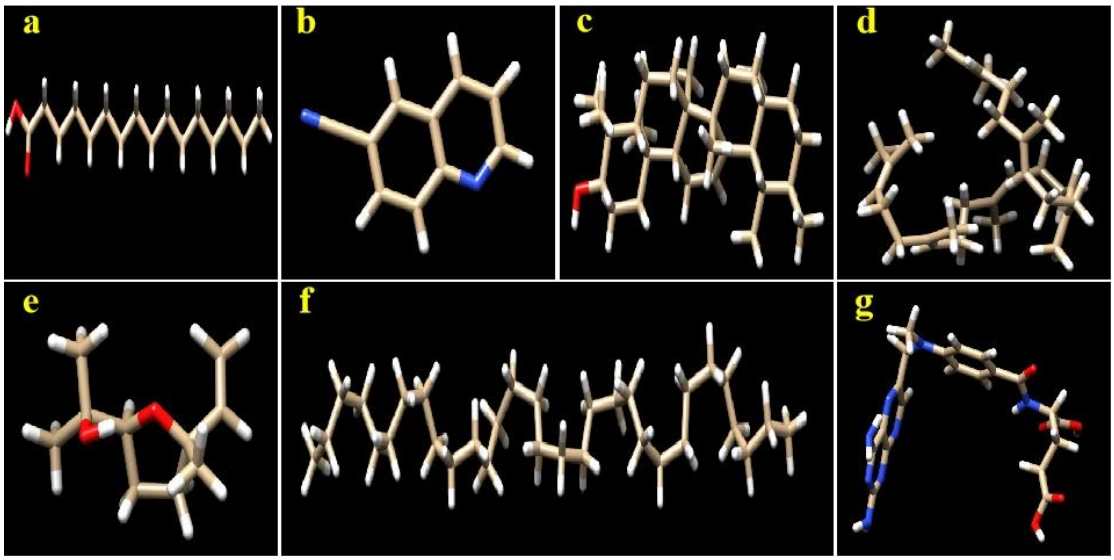

Figure 2. 3D structural representations of the compounds identified from the ethanolic flower extract of *C. indicum* and the reference drug: (a) n-Hexadecanoic acid (PubChem CID: 985), (b) 6-Cyanoquinoline (PubChem CID: 11373), (c) α-Amyrin (PubChem CID: 73170), (d) Supraene (PubChem CID: 134988859), (e) trans-Linalool (PubChem CID: 6429054), (f) Hentriacontane (PubChem CID: 12410), and (g) Methotrexate (standard drug; PubChem CID: 126941).

Table 1. Grid box parameters selected for cancer target protein, based on the binding site residues

PDB ID	Active Site Residues	Grid Box Parameter	
Rb	PHE A 293, CYS A 291, MET A 290,LEU A 289,LYS C 874,ARG C 876,LEU C 875,PHE C 877,PHE C 257,LEU A 106,ALA A 128,TYR ASN B 124,TYR B 134,PHE B 118,CYS B 171,HIS B 173,PHE B 152,LEU B 201,VAL B 223,LEU B 204,SER B 224,GLY B 228	33.576x13.979x21.171	84x58x64

***In vitro* Cytotoxicity Assessment by MTT Assay on Y79 Cell Line**

Cytotoxicity Assay (MTT Assay)

The Y79 human retinoblastoma cell line was obtained from the National Centre for Cell Science (NCCS) in Pune, India. Cells were inoculated in 96-well plates at a density of 3×10^4 cells per well and grown in serum-free RPMI media enriched with a 1× antibiotic-antimycotic solution. Following 24 hours of incubation at 37°C in a humidified environment with 5% CO_2, the cells were administered various amounts of the ethanolic flower extract of C. indicum (25, 50, 100, 125, and 150 µg/mL). Doxorubicin (2 µg/mL) served as the positive control. Following treatment, the culture media was discarded, and the cells were incubated with a 0.5 mg/mL MTT solution formulated in PBS for 4 hours. The MTT solution was thereafter removed, and the cells were meticulously rinsed with 200 µL of PBS. To dissolve the formazan crystals, 100 µL of DMSO was introduced to each well. Absorbance was measured at 570 nm with a microplate reader, and cell viability % was determined. The dose response relationship was employed to ascertain the optimum concentration and the half-maximal inhibitory concentration (IC_{50}) of the extract.

Acridine Orange/Ethidium Bromide (AO/EB) Staining

The Y79 human retinoblastoma cell line was inoculated in 12-well plates and cultured overnight at 37°C in a CO_2 incubator to facilitate cell adhesion. Cells were subsequently exposed to the ethanolic flower extract of *C. indicum* at its IC_{50} concentration for durations of 24 hours and 48 hours. Following treatment, 1 µL of a dual fluorescent staining solution containing acridine orange (100 µg/mL) and ethidium bromide (100 µg/mL) was introduced to each well and incubated for 30 minutes at ambient temperature. The cells were then rinsed twice with

sterile PBS. Apoptotic morphological changes, including chromatin condensation, nuclear fragmentation, and membrane blebbing, were observed under a fluorescence microscope within 20 min of staining.

Cell Cycle Analysis by Flow Cytometry

The cell cycle distribution of Y79 human retinoblastoma cells was evaluated after treatment with the ethanolic flower extract of *C. indicum*. Y79 cells were cultured in serum-free RPMI medium that was supplemented with a 1× antibiotic–antimycotic solution at a density of 2×10^6 cells/mL in 96-well plates. They were incubated for 24–48 hours at 37°C in a humidified 5% CO_2 atmosphere. The cells were treated with the extract at its IC_{50} concentration (118.07 µg/mL) for 24 hours. Following treatment, cells were then harvested, washed twice with sterile PBS, and centrifuged at 1500 rpm for 5 minutes. The cell pellets were fixed by adding ice-cold 70% ethanol dropwise and had been stored for 30 min at 4°C. After fixation, the cells were washed twice with PBS and were resuspended in a binding buffer that contained RNase A (100 µg/mL), FITC–Annexin V, and propidium iodide (PI, 100 µg/mL). Following a 15-minute incubation in the dark at room temperature, the samples were promptly analyzed by flow cytometry using a BD FACS Canto II (BD Biosciences, USA) to ascertain the proportion of cells in various cell cycle phases.

DNA Fragmentation Assay on Y79 Retinoblastoma Cells

DNA fragmentation analysis was used to determine apoptotic DNA cleavage in Y79 human retinoblastoma cells. Cells were maintained in RPMI-1640 media with 10% FBS and antibiotics at 37°C in a humidified environment with 5% CO_2. Approximately 1×10^6 cells/well were seeded onto six-well plates and allowed to adhere for 24 hours. The cells were treated with the ethanolic flower extract of *C. indicum* at its IC_{50} concentration and then incubated. After treatment, cells were collected, washed in PBS, and lysed in 500 µL of lysis buffer for 1 hour. Genomic DNA was extracted using the phenol: chloroform: isoamyl alcohol technique, then precipitated in cold isopropanol, air-dried, and rehydrated in distilled water. The concentration and purity of DNA were measured using a spectrophotometer. For fragmentation analysis, materials were resolved on a 0.8% agarose gel with a 100 bp DNA ladder, and the DNA banding pattern was observed using a gel documentation system (Bio-Rad, USA).

Statistical Analysis

All *in vitro* experiments were performed in triplicate and repeated at least three times. Statistical analysis was done using SPSS v17.0, with $p < 0.01$ considered significant.

RESULTS AND DISCUSSION

The qualitative phytochemical analysis of the ethanolic flower extract of *C. indicum* showed the presence of various bioactive secondary metabolites (Table 2). The extract showed a strong positive reaction (++) for alkaloids, terpenoids, phenolic compounds, flavonoids, and quinones, suggesting that these metabolites are present in significant quantities in the extract. Conversely, saponins, cardiac glycosides, and steroids were found to be moderately present (+). The results indicate that the ethanolic extract of C. indicum flowers is notably abundant in alkaloids, flavonoids, terpenoids, and phenolic compounds, which are recognized for their pharmacological properties, such as antioxidant, anti-inflammatory, and anticancer effects. The varying presence of phytochemicals underscores the potential of this extract as a source of therapeutic agents. Phytochemical screening revealed the presence of several secondary metabolites, including alkaloids, proteins, carbohydrates, phenols, saponins, flavonoids, tannins, and steroids could be responsible for certain biological activities of the extract (Rehman *et al*., 2023). Similar results have been observed in other medicinal plants, where initial phytochemical analysis consistently revealed alkaloids, flavonoids, phenolics, tannins, and terpenoids as key classes that contribute to their therapeutic potential (Prerna *et al.,* 2024).

Table 2. Qualitative analysis of phytochemicals from *C. indicum* flower ethanol extracts.

SL. No.	Phytochemical	Analyzing method	Ethanol extract
1	Alkaloids	Mayer's test	++
2	Terpenoids	Copper acetate test	++
3	Phenolic	Ferric chloride test	++
4	Saponins	Foam test	+
5	Flavonoids	Lead acetate test	++
6	quinines	NaOH test	++
7	Cardiac glycosides	Keller killani's test	+
8	steroids	H2SO4 Test	+

Highly Present (++), Present (+)

The ethanolic flower extract of *C. indicum* showed a concentration-dependent ability to reduce ferric ions, with FRAP values between 52.3 and 202.9 mg GAE/g (Figure 3) A robust linear correlation was noted between extract concentration and reducing power (R^2 = 0.9959), suggesting the existence of powerful electron-donating phytochemicals. The determined IC_{50} value of approximately 150 µg/mL indicates that the extract possesses a moderate-to-high antioxidant potential, highlighting its significance as a promising natural antioxidant candidate for use in nutraceutical and pharmaceutical fields. The phosphomolybdenum method, a recognized assay for assessing total antioxidant capacity, was utilized to analyze the ethanolic flower extract of *C. indicum*. The extract showed an increase in antioxidant activity that depended on its concentration, measured in ascorbic acid equivalents (AAE). A robust linear correlation (R^2 = 0.9836) validated the reliability of the response. The determined IC_{50} value (~106.78 µg/mL) indicates a moderate level of antioxidant potential when compared to standard antioxidants such as ascorbic acid and gallic acid (Figure 4). The findings indicate that the extract includes electron-donating bioactive compounds that can reduce Mo (VI) to Mo(V), thus affirming its role in total antioxidant capacity.

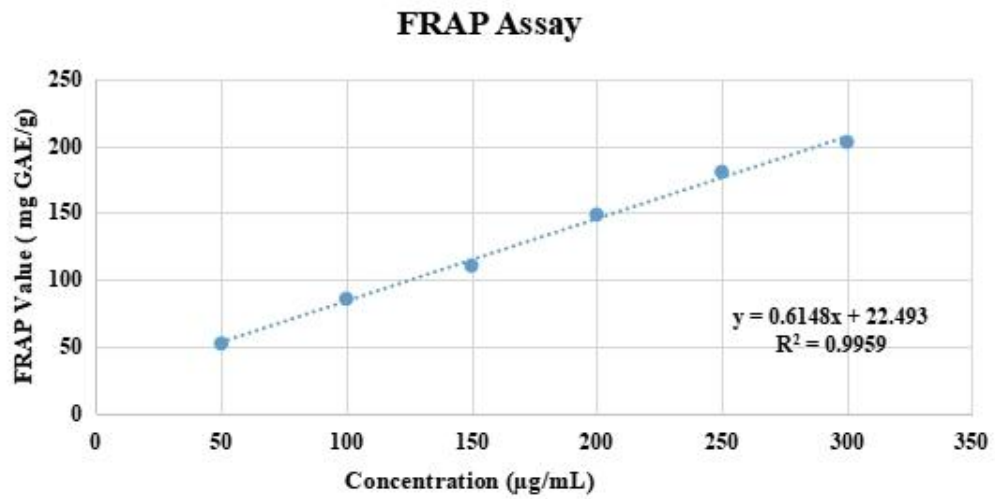

Figure 3. Antioxidant activity curve of FRAP method analysis Ethanolic flower extract of *C. indicum.*

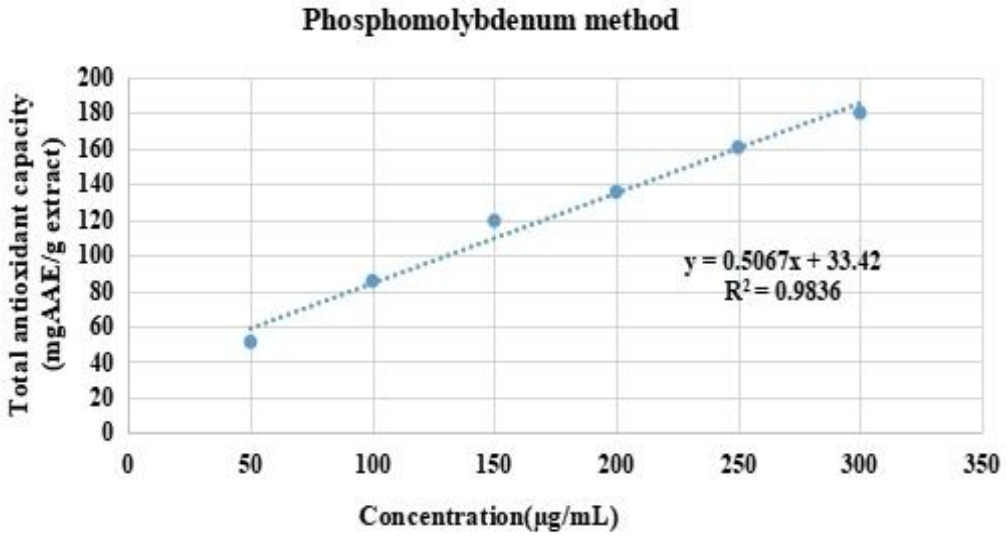

Figure 4. Antioxidant activity curve of Phosphomolybdenum analysis Ethanolic flower extract of *C. indicum.*

The findings demonstrate a consistent increase in antioxidant activity with longer extraction durations. Extended extraction time enhances the release of various bioactive compounds, particularly phenolic compounds, which are widely recognized for their antioxidant properties (Yusof *et al.,* 2021). In the DPPH radical scavenging assay, the plant extract displayed dose-dependent antioxidant activity, with an IC_{50} value of 48.87 µg/ml. In comparison, the standard ascorbic acid exhibited a stronger activity, with an IC_{50} of 21.14 µg/ml (Bhuiya, 2020). Recent investigations have further confirmed these findings, with antioxidant evaluation using the FRAP method showing that ethanolic extracts of plant flowers exhibited an IC_{50} value of 26.7 µg/mL, highlighting their strong reducing capacity (Kepel *et al.,* 2025). The results indicate that the antioxidant potential of Combretum flowers is mainly due to their rich phenolic and flavonoid content, confirming their importance as a valuable natural source of therapeutic antioxidants.

The primary phytoconstituents found in the ethanolic flower extract of *C. indicum*, including n-hexadecanoic acid, 6-cyanoquinoline, α-amyrin, supraene, trans-linalool, and hentriacontane, were selected for molecular docking studies following GC–MS profiling (Sidharth *et al.,* 2024). Docking experiments were conducted utilizing AutoDock Vina and Biovia Discovery Studio Client 2020 to evaluate their interaction with the retinoblastoma (Rb) protein (PDB ID: 3N5U), an essential regulator of cell cycle progression and tumor suppression. The most advantageous conformations were assessed by taking into account hydrogen bonding, hydrophobic interactions, van der Waals forces, and electrostatic contributions to the stability of protein-ligand complexes. The docking results (Table 3) indicated that α-amyrin (L3) exhibited the highest binding affinity (–8.6 kcal/mol), compared to the standard drug methotrexate (D1; –7.4 kcal/mol). This indicates that α-amyrin might have considerable inhibitory effects on Rb. Moderate binding energies were noted for 6-cyanoquinoline (L2; –6.4 kcal/mol), supraene (L4; –5.7 kcal/mol), and trans-linalool (L5; –5.4 kcal/mol), suggesting a partial but nevertheless significant interaction with the protein. On the other hand, n-hexadecanoic acid (L1; –4.0 kcal/mol) and hentriacontane (L6; –3.4 kcal/mol) showed relatively weak affinities. The findings collectively underscore α-amyrin as the most promising lead molecule among the phytocompounds studied, indicating its potential as a novel anticancer candidate targeting the Rb pathway. The moderate activity of other compounds indicates potential synergistic roles that could improve the therapeutic value of C. indicum extracts in cancer treatment.

Table 3. Docking scores of the three compounds from the ethanolic flower extract of *C. indicum* against Rb (PDB: 3N5U) cancer protein along with the standard drugs.

		Receptor (PDB ID)
Ligand (Drug)	**Code**	**3N5U**
n-Hexadecanoic acid	L_1	-4
6-Cyanoquinoline	L_2	-6.4
Alpha amyrin	L_3	-8.6
Supraene	L_4	-5.7
Trans-Linalool	L_5	-5.4
Hentriacontane	L_6	-3.4
Methotrexate (Standard Drugs)	D_1	-7.4

In the 3N5U protein–ligand complex, diverse interaction patterns were identified between the ligands and surrounding amino acid residues (Table 4). Ligand L1 forms two hydrogen bonds with GLU 56A (3.06 Å) and GLU 116A (1.98 Å) and establishes hydrophobic contacts with GLN 49A, LEU 53A, GLU 56A, and two PHE 119A residues, with interaction distances ranging from 3.67 to 3.91 Å (Figure 5). Ligand L2 (Figure 6) exhibits a broader hydrogen-bonding profile, engaging ARG 96A, ASN 124A, HIS 125A, two ARG 132B interactions, TYR 134A, and ARG 221A, with bond lengths between 2.34 and 3.06 Å, and additionally forming a hydrophobic contact with TYR 134A (3.85 Å). Ligand L3 establishes a strong hydrogen bond with ARG 23A (2.27 Å) and hydrophobic interactions with PRO 24A, GLN 68A, two TYR 70A residues, and ASN 271A (Figure 7). In contrast, ligand L4 does not form hydrogen bonds but interacts hydrophobically with GLN 181A, TRP 216A, two GLU 230A residues, VAL 231A, two LYS 234A residues, two PHE 235A residues, and LYS 238A, at distances between 3.55 and 3.90 Å (Figure 8). Ligand L5 forms a hydrogen bond with ARG 132B (2.44 Å) and hydrophobic interactions with ILE 130A, ILE 133B, TYR 134A, two TRP 206A residues, and ARG 221A (Figure 9). Ligand L6, although lacking hydrogen-bonding partners, participates in hydrophobic interactions with LEU 176A, TRP 216A, LYS 234A, two PHE 235A residues, and two LYS 238A residues (Figure 10). Finally, Ligand D1 (Standard drug)

forms multiple hydrogen bonds with ASN 124B, TYR 134B, and two GLN 249B residues, with bond lengths ranging from 2.13 to 3.13 Å, alongside hydrophobic interactions involving ASP 220B and ARG 221B (Figure 11). Overall, these findings emphasize the critical roles of ARG, TYR, and GLU residues, as well as aromatic residues such as PHE and TRP, in mediating hydrogen bonding and hydrophobic stabilization of ligand binding within the 3N5U complex. According to these results, alpha-amyrin (L3) and 6-cyanoquinoline (L2) appear to be promising prospects for the creation of anticancer drugs with a wide range of therapeutic applications.

Table 4. Interaction of aminoacid residues with ligands at receptor sites.

Protein	Ligands	Amino acids involved and distance (Å)	
		Hydrogen-Binding Interaction	**Hydrophobic Interaction**
3N5U	L1	56A GLU (3.06), 116 A GLU (1.98)	49A GLN (3.67), 53A LEU (3.91), 56A GLU (3.85), 119A PHE (3.76), 11 9A PHE (3.70)
	L2	96A ARG (3.06),124A ASN (2.34), 125A HIS (2.35), 132B ARG (2.51), 132B ARG (2.57), 134A TYR (2.91), 221A ARG (2.94)	134A TYR (3.85)
	L3	23A ARG (2.27)	24A PRO (3.42), 68A GLN (3.93), 70A TYR (3.43), 70A TYR (3.30), 271A ASN (3.50)
	L4	_____	181A GLN (3.68), 216A TRP (3.69), 230A GLU (3.90), 230A GLU (3.85), 231A VAL (3.57), 234A LYS (3.69), 234A LYS (3.55), 235A PHE (3.73), 235A PHE (3.64), 238A LYS (3.80)
	L5	132B ARG (2.44)	130A ILE (3.99), 133B —ILE (3.69), 134A TYR (3.62), 206A TRP (3.62), 206A TRP (3.68), 221A ARG (3.79)
	L6	_____	176A LEU (3.60), 216ATRP (3.68), 234A LYS (3.49) 235A PHE (3.49), 235A PHE (3.65), 238A LYS (3.63), 238A LYS (3.79)
	D1	124B ASN (2.13), 134B TYR (2.55), 249B GLN (2.92), 249B GLN (3.13)	220B ASP (3.82), 221B ARG (3.64)

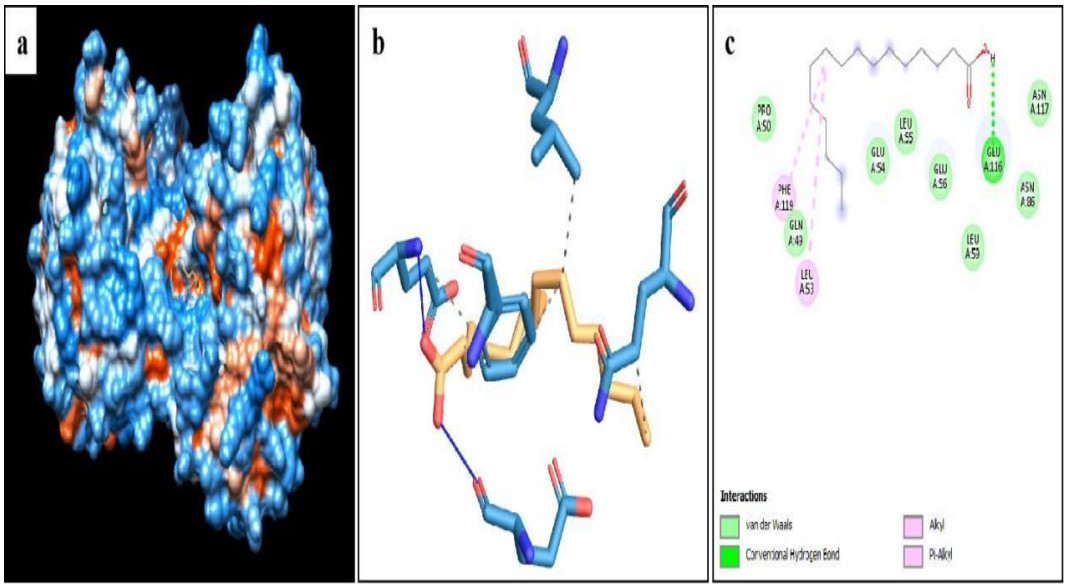

Figure 5. Surface model of target proteins Rb (PDB: 3N5U) with L1-n-Hexadecanoic acid molecular interaction (a) and interaction pose of inhibitors illustrating hydrogen bonds, van der Waal's forces, alkyl, Pi-alkyl and Pi-sigma at the binding pocket of L1 (b) and (c) with Rb protein.

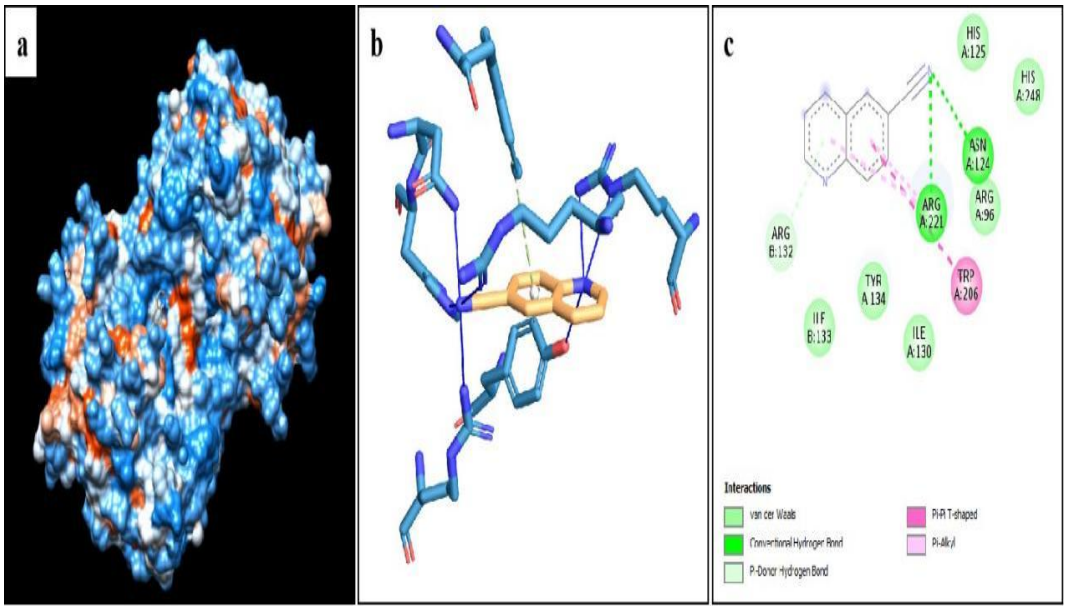

Figure 6. Surface model of target proteins Rb (PDB: 3N5U) with L2-6-Cyanoquinoline molecular interaction (a) and interaction pose of inhibitors illustrating hydrogen bonds, van der Waal's forces, alkyl, Pi-alkyl and Pi-sigma at the binding pocket of L1 (b) and (c) with Rb protein.

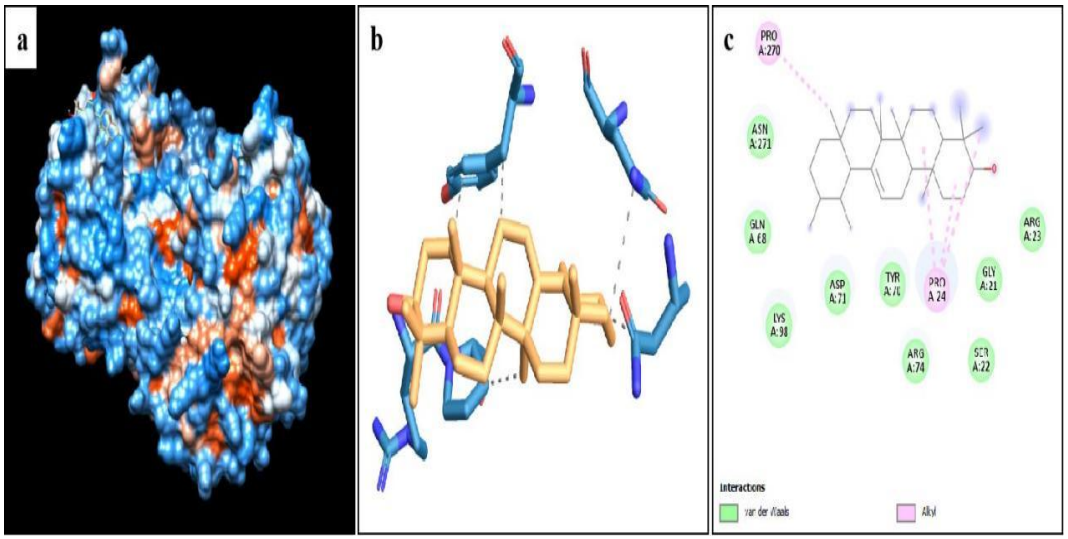

Figure 7. Surface model of target proteins Rb (PDB: 3N5U) with L3-Alpha amyrin molecular interaction (a) and interaction pose of inhibitors illustrating hydrogen bonds, van der Waal's forces, alkyl, Pi-alkyl and Pi-sigma at the binding pocket of L1 (b) and (c) with Rb protein.

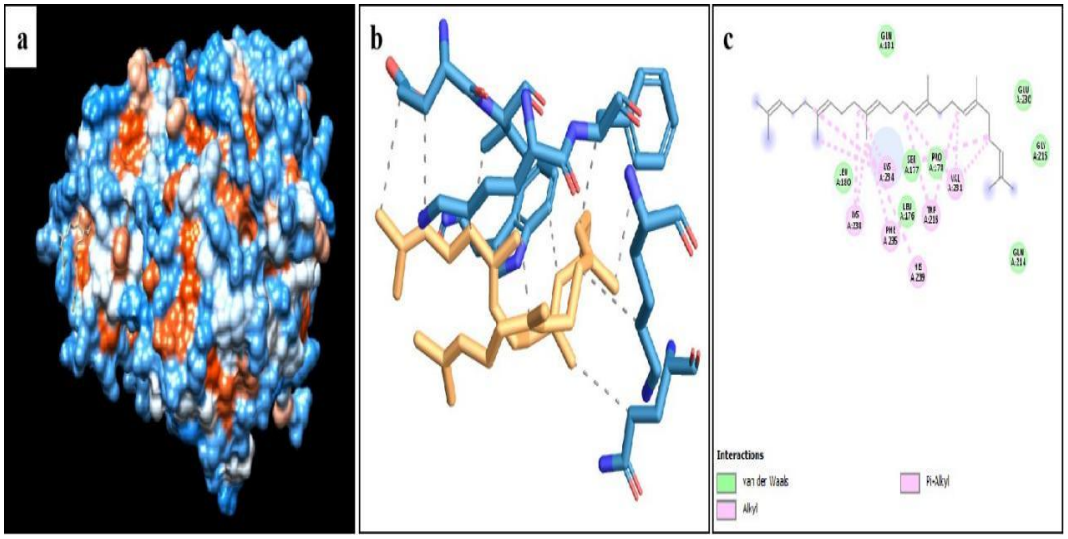

Figure 8. Surface model of target proteins Rb (PDB: 3N5U) with L4-Supraene molecular interaction (a) and interaction pose of inhibitors illustrating hydrogen bonds, van der Waal's forces, alkyl, Pi-alkyl and Pi-sigma at the binding pocket of L1 (b) and (c) with Rb protein.

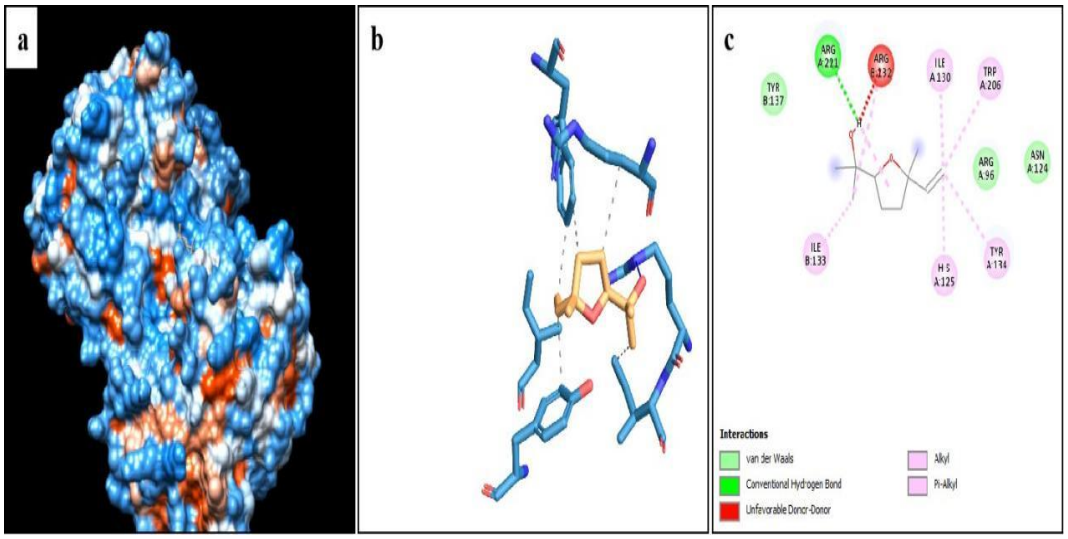

Figure 9. Surface model of target proteins Rb (PDB: 3N5U) with L5-Trans-Linalool molecular interaction (a) and interaction pose of inhibitors illustrating hydrogen bonds, van der Waal's forces, alkyl, Pi-alkyl and Pi-sigma at the binding pocket of L1 (b) and (c) with Rb protein.

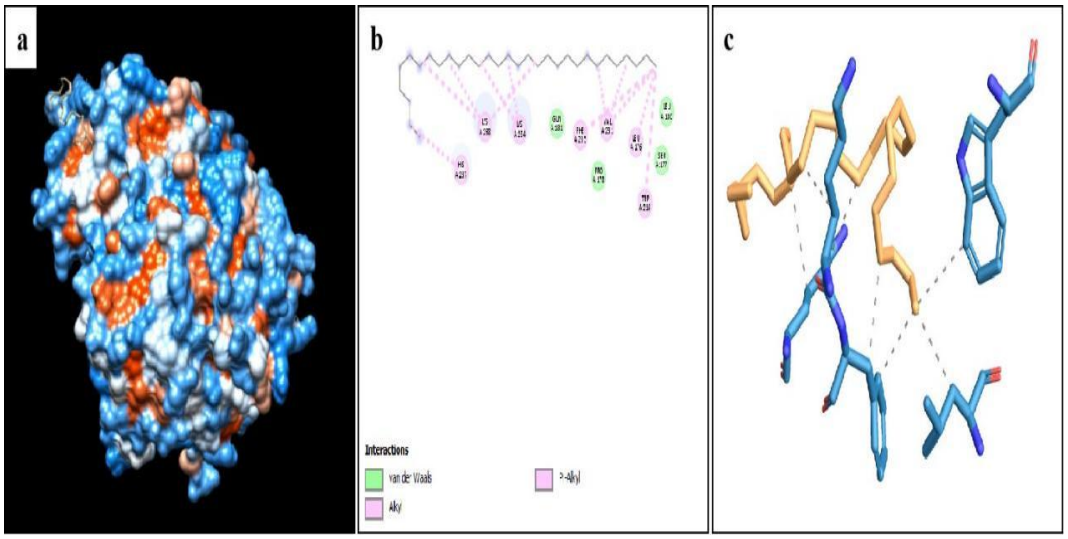

Figure 10. Surface model of target proteins Rb (PDB: 3N5U) with L6-Hentriacontane molecular interaction (a) and interaction pose of inhibitors illustrating hydrogen bonds, van der Waal's forces, alkyl, Pi-alkyl and Pi-sigma at the binding pocket of L1 (b) and (c) with Rb protein.

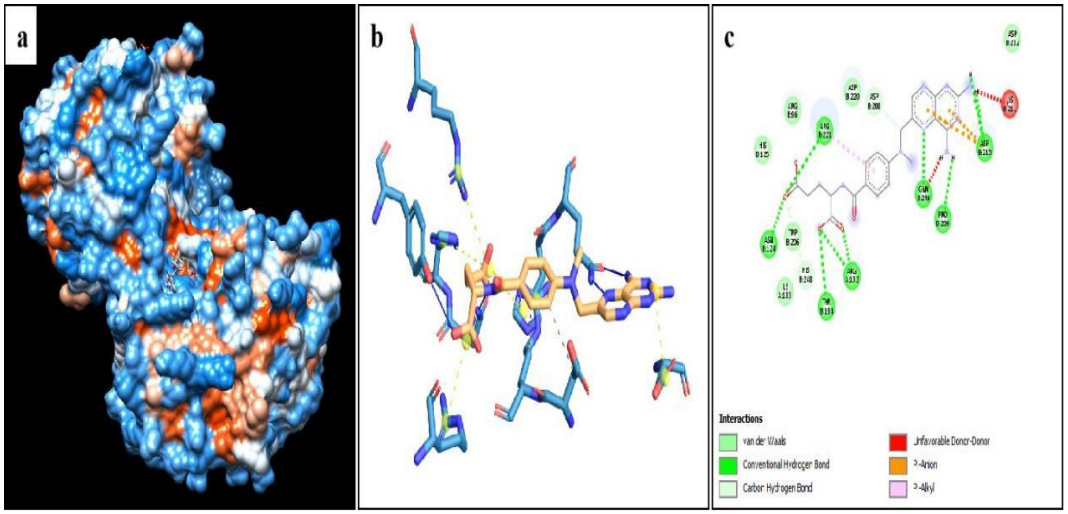

Figure 11. Surface model of target proteins Rb (PDB: 3N5U) with D1-Methotrexate molecular interaction (a) and interaction pose of inhibitors illustrating hydrogen bonds, van der Waal's forces, alkyl, Pi-alkyl and Pi-sigma at the binding pocket of D1 (b) and (c) with Rb protein.

This study's molecular docking analysis revealed that phytoconstituents from *C. indicum* engage with the retinoblastoma (Rb) protein mainly via hydrogen bonding and hydrophobic interactions. These interactions play a vital role in stabilizing ligands and provide important insights for creating new structure-based drugs (SBD) aimed at cancer treatment. Earlier research has indicated comparable results, showing that compounds derived from plants demonstrated consistent binding with proteins associated with cancer. Suhaibun *et al.* (2020) demonstrated the successful docking of garcinone E, triterpenoids, and gallic acid with p53, caspase-3, and Rb1, achieving docking scores of 3.873, 4.321, and 3.051, respectively. Elengoe and Loganthan (2022) showed that of the various protein–phyto-compound complexes studied, the Rb–quercetin interaction exhibited the highest stability with an affinity of –7.8 kcal/mol, outperforming the interactions of caspase-3 with quercetin and ferulic acid, as well as BRCA1 with both ferulic acid and quercetin. The results highlight the promise of flavonoids such as quercetin as potent inhibitors of cancer-related targets. Our findings align with previous docking studies indicating that α-amyrin, quercetin, and β-carotene from *Capparis zeylanica* exhibit a strong binding affinity (–8.4 kcal/mol) for the HER2 protein, as demonstrated using AutoDock Vina (Warake *et al.,* 2021).

In a similar vein, Sidharth *et al.* (2024) noted that significant components of ethanolic extracts—including n-hexadecanoic acid, 6-cyanoquinoline, α-amyrin, supraene, trans-linalool, and hentriacontane—demonstrated effective interactions with crucial cancer-related targets like CDK4 and CDK6, which play a direct role in the progression of retinoblastoma. In our docking study, α-amyrin demonstrated the highest binding affinity (–8.6 kcal/mol) with the Rb protein, surpassing the standard drug methotrexate. Recent evidence supports this observation, demonstrating that α-amyrin interacts strongly with several oncogenic targets, such as CDK4 (–7.5 kcal/mol), estrogen receptor (–9.5 kcal/mol), and EGFR (–8.7 kcal/mol) (Rosyadah *et al.,* 2025). The extensive binding capabilities highlight α-amyrin's potential as a strong candidate for anticancer treatment. The ethanolic flower extract of *C. indicum* showed a dose-dependent cytotoxic effect on Y79 retinoblastoma cells. The viability of cells showed a gradual decrease as the concentrations of the extract increased to 25, 50, 100, 125, and 150 µg/mL, leading to survival rates of 88.10 ± 0.90%, 75.60 ± 0.86%, 55.10 ± 0.95%, 42.70 ± 0.81%, and 34.40%, respectively (Figure 12). The determined IC_{50} value was 118.07 µg/mL, indicating notable cytotoxic effectiveness. At elevated concentrations, distinct morphological changes indicative of apoptosis was noted, such as the formation of apoptotic bodies, membrane rupture, cell rounding, and shrinkage (Figure 13). The results suggest that the extract causes cytotoxic effects in Y79 cells by disrupting their structure and viability, highlighting its potential as an anticancer agent.

The AO/EB dual staining demonstrated clear apoptotic characteristics in Y79 retinoblastoma cells after exposure to the ethanolic flower extract of *C. indicum*. Control cells that were not treated mainly showed a consistent green fluorescence, indicating that their membrane integrity was

intact and they were viable. Conversely, cells treated with the extract at its IC_{50} concentration (118.07 µg/mL) exhibited a higher proportion of orange-red fluorescence along with nuclear condensation, which is a sign of apoptosis (Figure 14). The staining effectively differentiated among viable, early apoptotic, late apoptotic, and necrotic populations, thus validating that the extract shows cytotoxic and anticancer properties by inducing apoptosis.

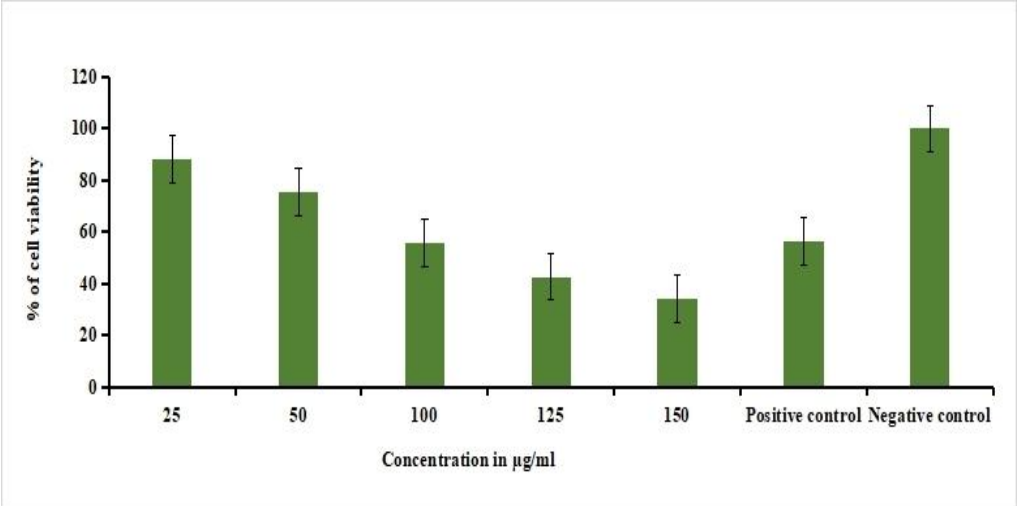

Figure 12. MTT analysis of *C. indicum* Ethanolic Flower Extract

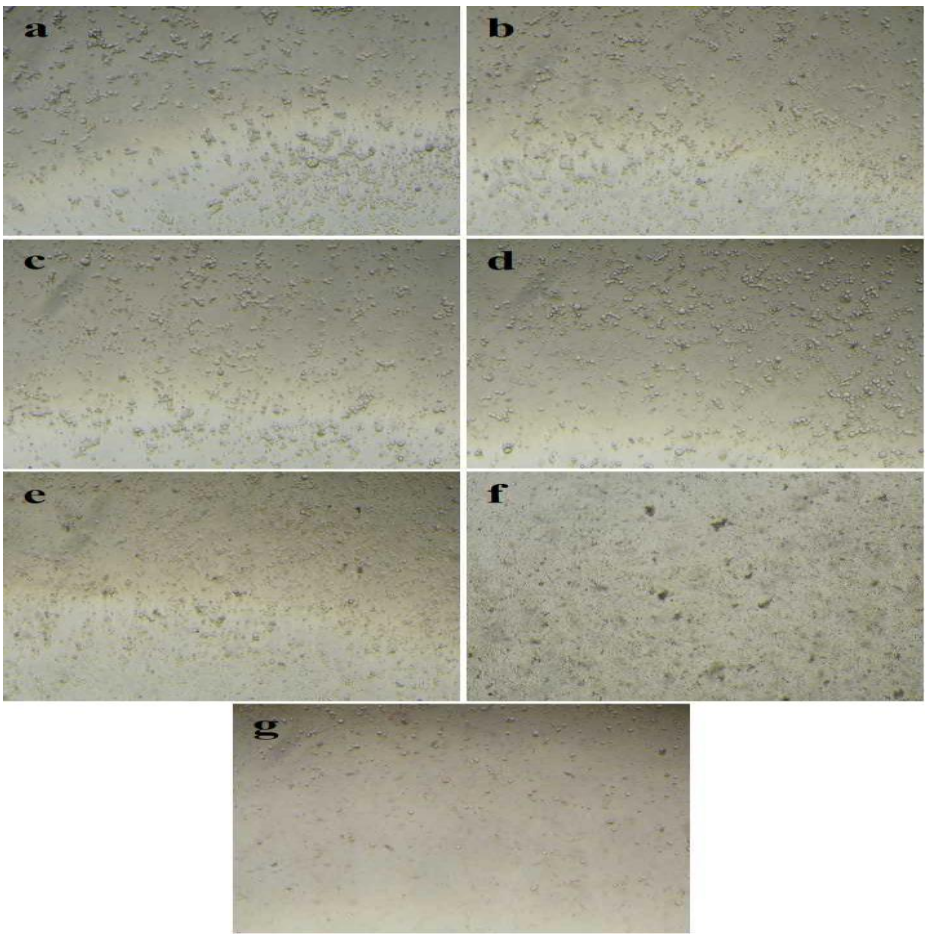

Figure 13. Morphological analysis of *C. indicum* Ethanolic Flower Extract treated Y79 cells for 24 hrs (a) Control (b)25 µg/ml (c) 50 µg/ml (d) 100 µg/ml (e) 125 µg/ml (f) 150 µg/ml (g) 2 µg/ml (Doxorubicin - Positive Control).

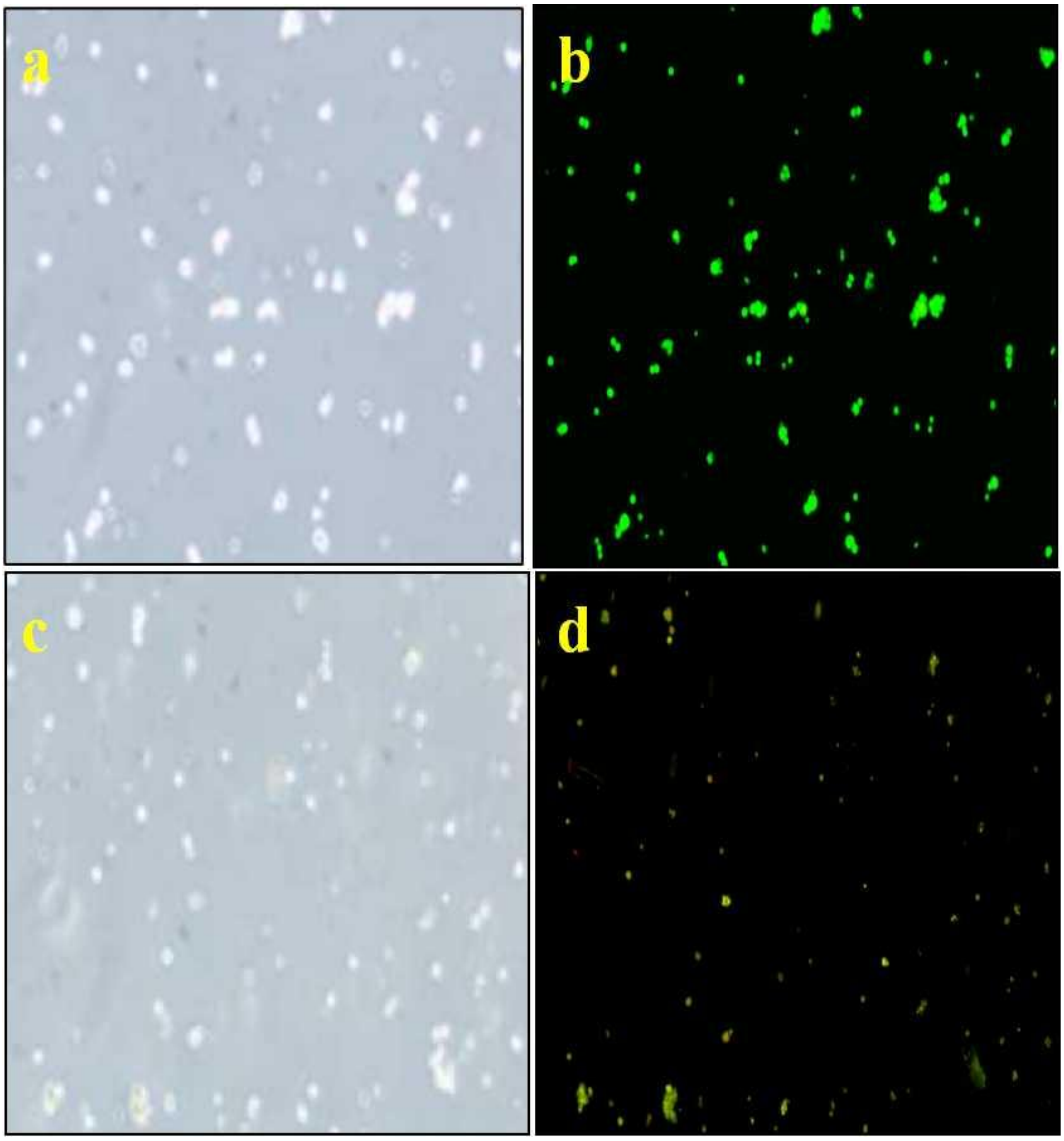

Figure 14. AO/EtBr staining assay of *C. indicum* Ethanolic Flower Extract treated Y79 cells (a and b) Control, (c and d) 118.07 µg/mL - IC_{50} Values

The ethanolic flower extract of *C. indicum* was found to significantly induce apoptosis in Y79 retinoblastoma cells, as demonstrated by Annexin V/PI staining. In the untreated control (Figure 15a), 98.6% of cells were viable, showing minimal necrosis at 0.5% and early apoptosis at 0.8%, with no late apoptotic population observed. In contrast, cells treated with the extract at its IC_{50} concentration (118.07 µg/mL) exhibited a significant decrease in viability (10.4%), along with rises in early apoptotic (15.6%) and late apoptotic (72.8%) populations (Figure 15b). The findings collectively indicate that the extract has a significant cytotoxic effect by enhancing apoptosis, mainly via late-stage apoptotic pathways, which plays a role in inhibiting the growth of Y79 cancer cells.

DNA fragmentation experiments further validated the triggering of apoptosis in Y79 retinoblastoma cells. As illustrated in Figure 16, DNA from untreated control cells remained intact, showing no signs of fragmentation, which indicates that apoptosis did not occur. On the other hand, cells that were treated with the ethanolic flower extract of *C. indicum* showed evident DNA fragmentation, which was shown by separate ladder-like bands and continuous smears. DNA ladders are a recognized sign of apoptosis, and the smearing pattern we observed supports systematic DNA cleavage as well. When examined together, these results strongly suggest that the extract causes Y79 cell death by fragmenting apart their genomic DNA.

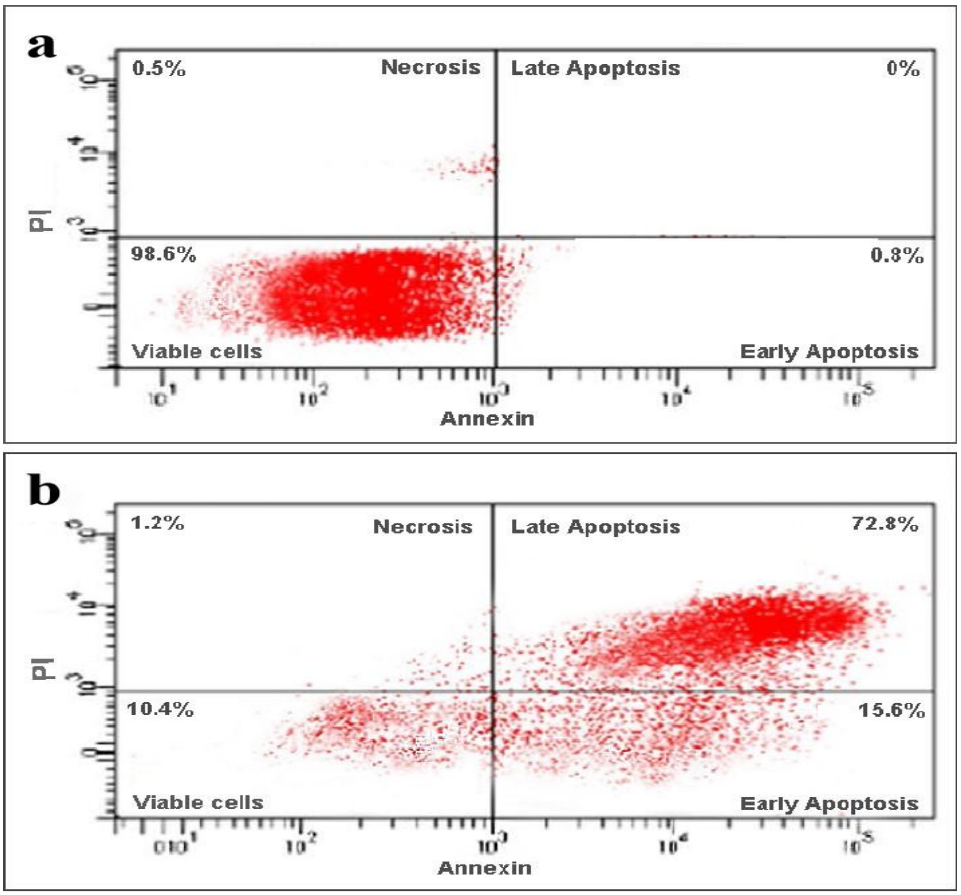

Figure 15. Apoptosis assay by flow cytometry using PI and Annexin V-FITC double staining method ethanolic flower extract (*Combretum indicum*) treated Y79 cells (a) Control, (b) 118.07µg/ml - IC_{50} Values.

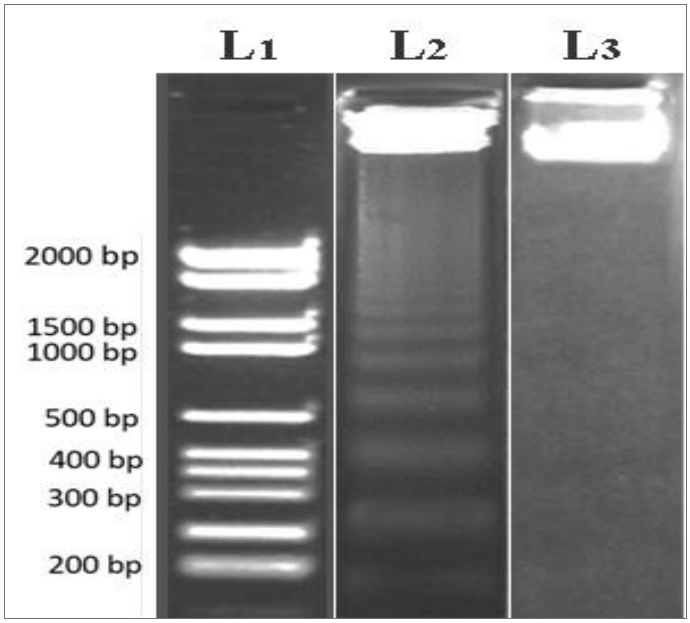

Figure 16. DNA fragmentation studies of ethanol flower extracts on Y79 cells. L1: 1kb Marker DNA L2: Fragmented DNA of Y79 cells after treating with ethanol extract of flower L3: DNA profile of Y79 cells (undigested).

Previous research provides compelling evidence for the wide-ranging anticancer effects of *C. indicum*, aligning with our observations in Y79 retinoblastoma cells. Plant-derived anticancer phytochemicals have the potential to delay the progression of normal cells into cancerous ones, promote the death of tumor cells, and inhibit processes such as angiogenesis and metastasis (Rahman and Khan, 2013). Research on *C. indicum* extracts has shown that different plant parts and extraction solvents yield varying degrees of cytotoxicity. The highest levels of cytotoxic activity were observed in extracts from the flower using petroleum ether and ethanol, and from the leaves using ethyl acetate, with the ethyl acetate flower extract demonstrating the most pronounced effect. Conversely, extracts from the roots and stems exhibited only minimal cytotoxicity (Mahajan *et al*., 2017). In tests on Ehrlich ascites carcinoma (EAC) cells, the whole plant extract significantly reduced cell viability in a dose-dependent manner. At higher concentrations, its cytotoxic effects were comparable to those of vincristine, a standard chemotherapy drug. These findings suggest that the aerial parts of *C. indicum* possess strong antioxidant and antitumor properties, supporting its potential use in complementary cancer therapies (Abd Elkarim and Taie, 2023). Additionally, the compounds Combretin A and Combretin B demonstrated anti-nociceptive, anti-inflammatory, and anticancer activities, likely through suppression of reactive oxygen species (ROS), tumor necrosis factor-alpha (TNFα), and nitric oxide (NO) production, indicating their promise as therapeutic agents for breast cancer and inflammatory conditions (Mbiantcha *et al*., 2018). *C. indicum* extracts have demonstrated cytotoxic effects in breast and hematological cancer models, in addition to hepatocellular and resistant cancer types. Hodaei *et al.* (2021) noted that methanolic extracts from the cultivars “Dorna2” and “Farhood” inhibited MCF-7 cell viability, with IC_{50} values approximately 312 µg/mL. In a similar vein, Kim *et al.* (2012) discovered that ethanolic and fractionated extracts showed considerable cytotoxicity in prostate (DU145) and multiple myeloma (U266) cells, although the effects were less pronounced in MDA-MB-231 breast carcinoma cells. Hairul *et al.* (2020) demonstrated that aqueous flower extracts effectively inhibited the proliferation of HL-60 leukemia cells in hematological cancers, with the effects observed to be both time- and dose-dependent. The IC_{50} values decreased from 320 µg/mL at 24 hours to 168 µg/mL at 72 hours. Morphological evidence, such as blebbing, shrinkage, and the formation of apoptotic bodies, confirmed that apoptosis is a crucial mechanism of action.

Other medicinal plants tested against retinoblastoma have shown similar observations. Kamarudin *et al.* (2022) showed that optimized ethanolic bulb extracts of *Eleutherine bulbosa* effectively inhibited the growth of retinoblastoma cells (IC_{50} = 15.7 µg/mL), while also inducing apoptosis, membrane blebbing, and G0/G1 cell cycle arrest. The results align with our observations regarding *C. indicum* flower extract, which similarly induced significant late apoptosis and DNA fragmentation in Y79 cells. The gathered evidence indicates that *C. indicum* holds promise as a natural source of anticancer agents that can induce apoptosis and inhibit proliferation, particularly in the context of retinoblastoma, where treatment options remain constrained.

CONCLUSION

This study demonstrates that the ethanolic floral extract of *C. indicum* is rich in bioactive phytochemicals, including alkaloids, flavonoids, terpenoids, and phenolic compounds, all of which play a role in its pharmacological properties. Antioxidant experiments demonstrated a moderate to high capacity for free radical scavenging and reducing potential, suggesting strong electron donation capabilities. Molecular docking experiments showed that α-amyrin and 6-cyanoquinoline are promising ligands, effectively binding to the retinoblastoma protein (3N5U) and stabilizing essential amino acid residues, suggesting their therapeutic potential. Further in vitro tests demonstrated a dose-dependent cytotoxic effect of the extract on Y79 retinoblastoma cells. AO/EB dual staining, Annexin V/PI flow cytometry, and DNA fragmentation reliably indicated that apoptosis, rather than necrosis, was responsible for cell death. The data indicate that the extract from *C. indicum* flowers, particularly its bioactive α-amyrin, could serve as a promising antioxidant and anticancer agent for the treatment of retinoblastoma.

ACKNOWLEDGMENT

The authors appreciate the lab facilities provided by the Department of Biochemistry, Sree Narayana Guru College, Coimbatore, Tamil Nadu, India, for providing laboratory facilities to conduct this research work.

CONFLICT OF INTERESTS

The authors declare no conflict of interest

ETHICS APPROVAL

Not applicable

FUNDING

This study received no specific funding from public, commercial, or not-for-profit funding agencies.

AI TOOL DECLARATION

The authors declares that no AI and related tools are used to write the scientific content of this manuscript.

DATA AVAILABILITY

Data will be available on request

REFERENCES

Abd Elkarim, A.S., & Taie, H.A. (2023). Characterization of flavonoids from *Combretum indicum* L. Growing in

Egypt as antioxidant and antitumor agents. *Egyptian Journal of Chemistry,* 66(13), pp.2291-2305.

Benzie, I. F. F., & Strain, J. J. (1996). The ferric reducing ability of plasma (FRAP) as a measure of antioxidant power: The FRAP assay. *Analytical Biochemistry*, 239(1), 70–76.

Bhuiya, N. M. A. (2020). Investigation on antioxidant and antimicrobial properties of methanolic extract of *Combretum indicum* leaf. *International Journal of Green Pharmacy (IJGP)*, 14(02).

Chaachouay, N., & Zidane, L. (2024). Plant-derived natural products: A source for drug discovery and development. *Drugs and Drug Candidates, 3*(1), 184–207. https://doi.org/10.5678/ddc.2024.3.1.184.

Dallakyan, S., & Olson, A.J. (2015) Small-molecule library screening by docking with PyRx. In: *Chemical Biology.* New York, NY: Humana Press. 243–50.

Dimaras, H., Corson, T. W., Cobrinik, D., White, A., Zhao, J., Munier, F. L., Abramson, D. H., Shields, C. L., Chantada, G. L., Njuguna, F., & Gallie, B. L. (2015). Retinoblastoma. *Nature Reviews Disease Primers, 1*(1), 1–23.

Doğan, S., Tuncer, M. C., & Özdemir, İ. (2025). Inhibition of retinoblastoma cell growth by boswellic acid through activation of the suppressing nuclear factor—κB activation. *Medicina, 61*(3), 480. https://doi.org/10.3390/medicina61030480.

Eberhardt, J., Santos-Martins, D., Tilack, A. F., & Forli, S. (2021). AutoDock VINA 1.2.0: New docking methods, expanded force field, and Python bindings. *Journal of Chemical Information and Modeling, 61*, 3891–3898.

Elengoe, A., & Loganthan, V. (2022). Molecular modeling and docking studies on phyto-compounds against caspase-3, BRCA1, and Rb. *Biointerface Research in Applied Chemistry, 12*, 7606–7620.

Gupta, V. B., Manjusha, R., Ravishankar, B., Harisha, C. R., Shukla, V. J., & Khant, D. B. (2012). Pharmacognostical and physicochemical analysis of Pathyadivarti–A polyherbal Ayurvedic formulation. *International Journal of Pharma and Life Sciences, 3*(4), 1643–1649.

Hairul, N. M., Zainuddin, H. Z. M., & Osman, W. N. W. (2020). Cytotoxic and morphological effects of *Chrysanthemum indicum* aqueous extracts of bud and flower on human acute promyelocytic leukemia (APL) HL-60 cell lines in vitro. *Asian Journal of Medicine and Biomedical Research, 4*(SI 1), 17–25.

Hodaei, M., Rahimmalek, M., & Behbahani, M. (2021). Anticancer drug discovery from Iranian *Chrysanthemum* cultivars through system pharmacology exploration and experimental validation. *Scientific Reports, 11*(1).

Jain, R., Sharma, S., & Jain, S. (2019). A review on phytochemical and pharmacological potential of *Combretum indicum*. *Journal of Drug Delivery and Therapeutics, 9*(4), 651–654.

Jin, L., Zhang, W., Pan, H., Li, T., Liu, B., Zhao, J., & Wang, B. (2017). Retrospective investigation of retinoblastoma in Chinese patients. *Oncotarget, 8*, 108492–108497.

Jin, Z. B., Xu, J., & Li, B. (2024). Reflection on the origin and pathogenesis of retinoblastoma. *Zhonghua Yan Ke Za Zhi, 60*, 883–886.

Kamarudin, A. A., Sayuti, N. H., Saad, N., Ab Razak, N. A., & Esa, N. M. (2022). Induction of apoptosis by *Eleutherine bulbosa* (Mill.) Urb. bulb extracted under optimised extraction condition on human retinoblastoma cancer cells (WERI-Rb-1). *Journal of Ethnopharmacology, 284*, 114770.

Kepel, B. J., Rotty, L. W., Tallei, T. E., & Nurkolis, F. (2025). Integrating in vitro and in silico techniques for evaluating the antioxidant activity of *Chrysanthemum indicum* L. *Pharmacia, 72*, 1–14.

Kim, C., Kim, M.C., Kim, S.-M., Nam, D., & Choi, S.-H. (2012). *Chrysanthemum indicum* L. extract induces apoptosis through suppression of constitutive STAT3 activation in human prostate cancer DU145 cells. *Phytotherapy Research, 27*(1), 30–38.

Mahajan, C. P., & Aher, A. N. (2017) A review on ethnobotanical, phytochemical and pharmacological activities of *Quisqualis indica* Linn. J *Pharmacogn Phytochem.* 2017;9(1):47-52.

Mbiantcha, M., Almas, J., Dawe, A., Faheem, A. & Sidra, Z. (2018). Analgesic, anti-inflammatory and anticancer activities of Combretin A and Combretin B isolated from *Combretum fragrans* F. HOFFM (Combretaceae) leaves. *Inflammopharmacology,* 26(6), pp.1429-1440.

Mishra, S. C., & Sharma, N. (2021). Qualitative and quantitative study of phyto constituents and antioxidant potential of rhizomes of Kaempferia galanga, Kaempferia parviflora and Kaempferia pulchra. *Journal of Pharmaceutical Research International,* 33(56A), 150–159.

Monica, M., Visagaperumal, D., & Chandy, V. (2024). Exploring the therapeutic potential of *Combretum indicum*: Bridging traditional wisdom with modern medicine. *International Journal of Modern Pharmaceutical Research, 8*(7), 127–132.

Moteriya, P., Satasiya, R., & Chanda, S. (2015). Screening of phytochemical constituents in some ornamental flowers of Saurashtra region. *Journal of Pharmacognosy and Phytochemistry, 3*(5), 112–120.

Nasim, N., Sandeep, I. S., & Mohanty, S. (2022). Plant-derived natural products for drug discovery: Current approaches and prospects. *The Nucleus, 65*(3), 399–411.

Pawar, S. S., & Rohane, S. H. (2021). Review on discovery studio: An important tool for molecular docking. *Asian Journal of Research in Chemistry, 14*, 86–88.

Prerna, Chaudhary, P., Farooqui, N. A., & Ahmad, S. (2024). Phytochemical investigation and assessment of in-vitro anti-inflammatory activity of hydroethanolic extracts of *Combretum indicum* and *Euphorbia milii*: A comparative study. *Journal of Chemical Health Risks, 14*(6), 401–413.

Rahman, M. M., & Khan, M. A. (2013) Anti-cancer potential of South Asian plants. *Nat. Prod. Bioprospecting.* 3, 74-88(2013).

Ramalingam, P. S., Priyadharshini, A., Emerson, I. A., & Arumugam, S. (2023). Potential biomarkers uncovered by bioinformatics analysis in sotorasib resistant–pancreatic ductal adenocarcinoma. *Frontiers in Medicine, 10*, 1107128.

Rehman, K.U., Ullah, S., Butt, Z.A., Muhammad, M., Yaseen, T., Khan, S.S. & Khan, A.A. (2023). Phytochemical Screening, Phytotoxic and Antimicrobial Prospective of Rangoon Creeper (*Combretum indicum* L.) Against Known Plants Bacterial and Fungal Pathogens: Prospective of Rangoon Creeper (*Combretum indicum L.*) Against Plants. *Biological Sciences-PJSIR,* 66(3), pp.220-229.

Rosyadah, N., Kamila, F. S., Hermanto, F. E., Widyananda, M. H., Grahadi, R., Dwijayanti, D. R., Widodo, N., & Ulfa, S. M. (2025). *Daruju* (*Acanthus ilicifolius* L.) may exhibit anti-breast cancer activity through inhibition of proliferation regulators: A computational study. *Journal of Tropical Life Science, 15*(1), 127–136.

Sidharth, K., Narayanasamy, K., & Mohan, S. (2024). GC-MS profiling and in silico potential bioactivity prediction of ethanolic extract of *Combretum indicum* (L.) against intraocular tumor-associated proteins. *African Journal of Biomedical Research, 27*(4s), 15773–15791.

Suhaibun, S. R., Elengoe, A., & Poddar, R. (2020). Technology advance in drug design using computational biology tool. *Malaysian Journal of Medicine & Health Sciences, 16*, 1–10.

Warake, R. A., Jarag, R. J., Dhavale, R. P., Jarag, R. R., & Lohar, N. S. (2021). Evaluation of in vitro antioxidant, anticancer activities and molecular docking studies of *Capparis zeylanica* Linn. leaves. *Future Journal of Pharmaceutical Sciences, 7*(1), 1–2.

Yadav, R. N. S., & Agarwala, M. (2011). Phytochemical analysis of some medicinal plants. *Journal of Phytology, 3*(12), 10–14.

Yanik, O., Gunduz, K., Yavuz, K., Tacyildiz N., &Unal E (2015) Chemotherapy in retinoblastoma: current approaches. *Turk Journal of Ophthalmology,* 45,259–67.

Yusof, N., Munaim, M. S. A., & Veloo Kutty, R. (2021). Optimization of total phenolic compounds extracted from propolis by ultrasound- assisted extraction. *Chemical Engineering Communications,* 208(4), 564-572.

Zhao, J. Y., Li, S. F., Shi, J. T., & Wang, N. L. (2011). Clinical presentation and group classification of newly diagnosed intraocular retinoblastoma in China. *British Journal of Ophthalmology, 95*, 1372–1375.